



ELSEVIER

Journal of Volcanology and Geothermal Research 102 (2000) 169–187

Journal of volcanology
and geothermal research

www.elsevier.nl/locate/jvolgeores

Seismic phenomena associated with the 1996 Vatnajökull eruption, central Iceland

K.I. Konstantinou^{a,*}, G. Nolet^b, W.J. Morgan^b, R.M. Allen^b, M.J. Pritchard^a

^aDepartment of Geological Sciences, University of Durham, South Road, Durham DH1 3LE, UK

^bDepartment of Geosciences, Guyot Hall, Princeton University, Princeton, NJ 08544, USA

Received 15 September 1999; received in revised form 23 February 2000; accepted 23 February 2000

Abstract

During late September 1996, a major eruption took place at the NW part of the Vatnajökull glacier in central Iceland. The eruption was preceded by intense seismic activity, which began with a $M_w = 5.6$ earthquake two days previously. Two very active volcanic systems, Bárðarbunga and Grimsvötn, are situated in that area underneath the permanent ice cap. The volcano-seismic phenomena associated with the eruption were recorded on both temporary (HOTSPOT) and permanent (SIL) seismic networks, covering most parts of the country. The recorded events were categorised, according to their waveform shape and frequency content, into three groups: (1) low-frequency events; (2) mixed-frequency events; and (3) volcanic tremor. The large earthquake at Bárðarbunga volcano, which initiated the seismic activity before the eruption, was located inside the caldera and had the characteristics of a non-double couple event. The epicentres of the earthquake swarm that followed it initially delineated the caldera rim and then migrated towards Grimsvötn, possibly indicating lateral movements of magma from a shallow chamber beneath Bárðarbunga. The eruption affected an area much larger than that between these two volcanoes, since seismic activity was also observed at distances 20 km away, at the Tindafjallajökull volcanic system. The spectral analysis of tremor, recorded at the nearest station to the eruption site, revealed its existence before the onset of the eruption in five narrow frequency bands (0.5–0.7, 1.6, 2.2, 2.8, 3.2 Hz) representing fundamental frequencies with their half- and quarter-subharmonics. This pattern continued until the last day of the eruption. It is believed that the eruption was caused by a dyke injection that had been going on beneath the Vatnajökull area for a period of 10 years. © 2000 Elsevier Science B.V. All rights reserved.

Keywords: Vatnajökull glacier; low-frequency events; mixed-frequency events; volcanic tremor; non-double couple event; dyke injection

1. Introduction

The NW part of the Vatnajökull glacier (Fig. 1) has been the centre of intense volcanic and seismic activity in historical times (Einarsson and Brandsdóttir, 1984; Björnsson and Einarsson, 1990; Gudmundsson and Björnsson, 1991) and is also suggested by geophysical (Einarsson, 1954; Tryggvason et al.,

1983;) and geochemical studies (Sigvaldasson et al., 1974) as the centre of the Icelandic hotspot. The fact that the area is covered by a thick ice layer and that it is tens of kilometres away from the inhabited south coast has made it difficult to resolve structural details of the volcanic systems that lie underneath the ice cap. Two of these volcanic systems, responsible for much of the observed activity, are Bárðarbunga and Grimsvötn. Each is characterised by an elliptical shape caldera structure and it is generally believed that the fissure swarms that appear outside the ice cap

* Corresponding author. Fax: + 44-191-374-2510.

E-mail address: konstantinos.konstantinou@durham.ac.uk (K.I. Konstantinou).

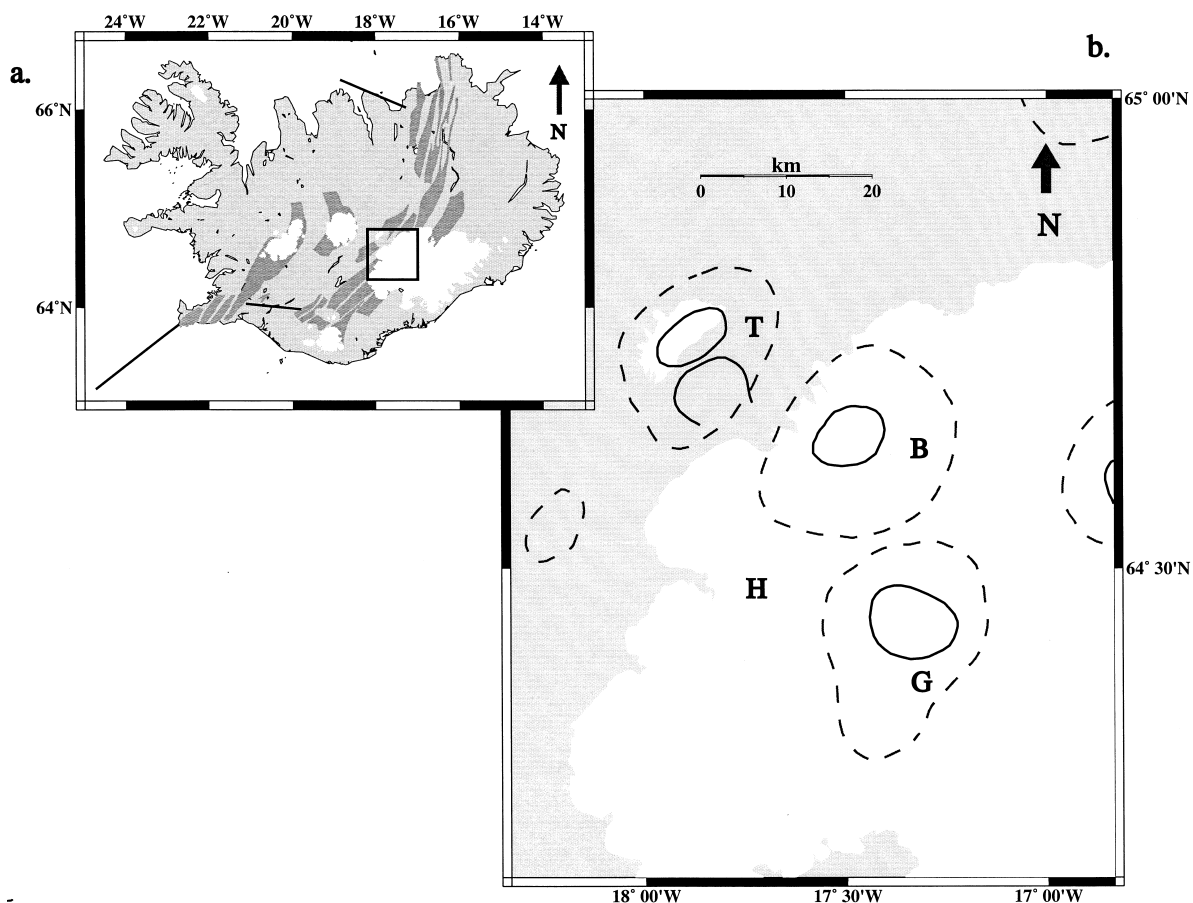


Fig. 1. (a) Map of the neovolcanic and fracture zones in Iceland. The square shows the area where the Vatnajökull eruption took place. White areas indicate permanent glaciers. (b) Map of the NW part of the Vatnajökull glacier. Solid lines represent the outline of calderas, dashed lines represent the outlines of central volcanoes. T: Tindafjallajökull; B: Bárðarbunga; G: Grimsvötn; H: Hamarinn.

are connected to these volcanic systems (Sæmundsson, 1979, 1980; Jakobsson, 1979, 1980).

Over the last 1100 years, the volcanoes beneath Vatnajökull are believed to have erupted 80 times,

with 63 eruptions considered as certain, of which the number of eruptions at Grimsvötn has been estimated between forty and fifty (Gudmundsson and Björnsson, 1991). During this century, Grimsvötn

Table 1

Eruptions in the Grimsvötn area over the last century (after Gudmundsson and Björnsson, 1991)

Year	Duration	Associated phenomena	Volume erupted (km ³)
1934	≥ 2 weeks	Depressions in the ice, jökulhlaup	0.03–0.04
1938	1–5 weeks	7–8 km fissure, jökulhlaup	0.3–0.5
1983	5–6 days	Depression in the ice	0.01
1984	1 h?	Volcanic tremor recorded	?
1996	2 weeks	9 km fissure, jökulhlaup	0.4
1998	10 days	Depressions in the ice	?

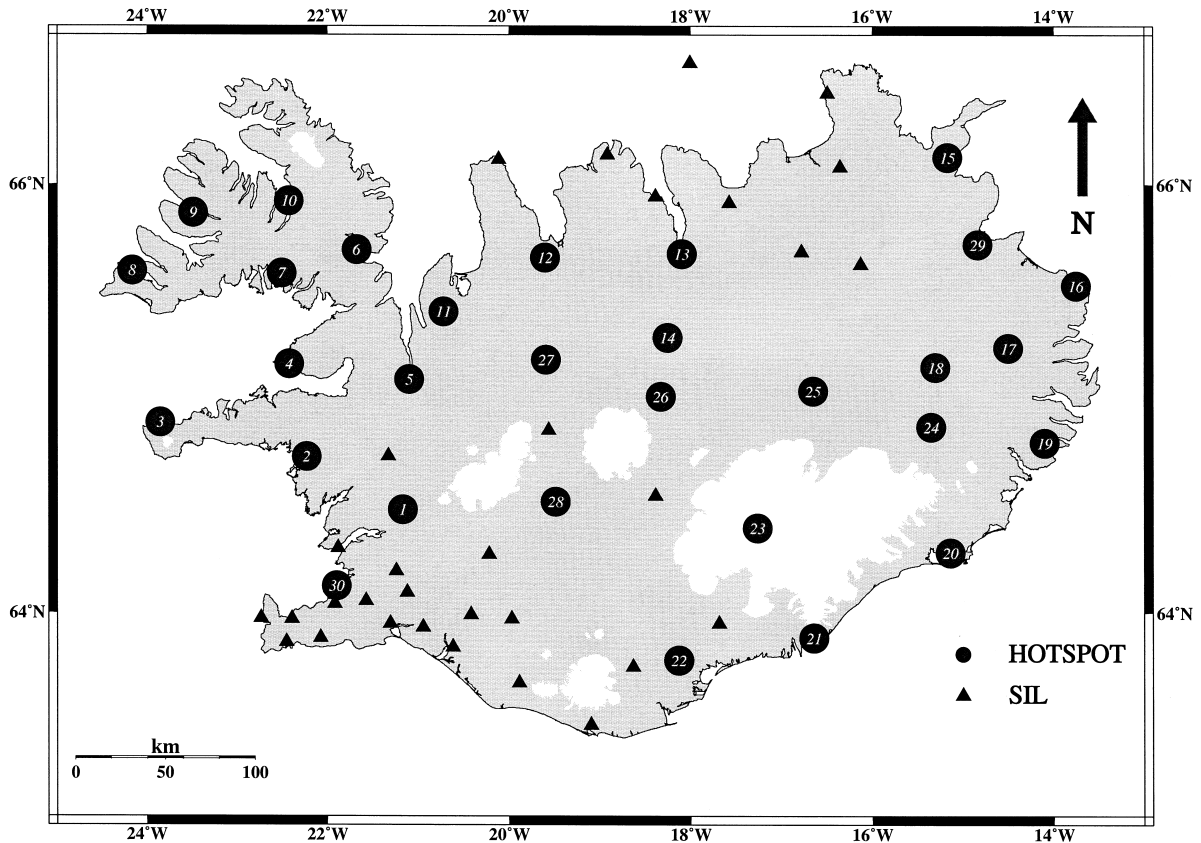


Fig. 2. Map of the HOTSPOT and SIL seismic networks.

has erupted six times (Table 1), including the latest eruption on 18 December 1998, after the large eruption in 1996. Most of the information that we have about the eruptive activity in Grimsvötn come from aerial photographs of the area. Such observations show openings in the ice shelf or depressions in the ice at the eruption site, filled with meltwater produced by the interaction of magma with ice. Accumulation of meltwater in the Grimsvötn caldera and its subsequent drainage underneath the glacier to the south coast has caused in the past catastrophic floods, that are described in the literature with the term “jökulhlaup” (meaning flooding from the glacier). However, jökulhlaups cannot be considered as definite indicators of eruptions, since the high geothermal heat flux may also cause excessive production of meltwater (Björnsson, 1988).

Several geophysical studies have been carried out in the Grimsvötn area, including radio echo-sounding

(Björnsson and Einarsson, 1990) and seismic reflection surveys (Joset and Holtzschler, 1954; Gudmundsson, 1989). They revealed an ice thickness of 240–260 m and a permanent subglacial caldera lake covering an area of 10 km² with a water depth of 40–90 m. The caldera floor was found to be covered by sediments in the northern and eastern parts and with lava flows in its southern part (Gudmundsson, 1989).

The first eruption in Grimsvötn to be detected by an increase in the level of seismicity was that of 1983, when a seismic network of 35 stations throughout the country was fully operational. The eruption was preceded by an intense earthquake swarm, believed to have been caused by the failure of the magma chamber walls and subsequent migration of magma in the surface (Einarsson and Brandsdóttir, 1984). Volcanic tremor was also recorded and it was most intense during the first 12 h of the eruption. Tremor

was observed again one year later, on 21 August 1984 for only 1 h and was interpreted as a small eruption that did not reach the surface of the ice (Björnsson and Einarsson, 1990).

Unlike Grimsvötn, Bárðarbunga was identified as an active volcano only recently, when aerial photographs revealed its elliptical shaped caldera (Einarsson, 1991). There are no historical records of volcanic activity in Bárðarbunga, even though tephrochronological and geochemical studies suggest that it may have been active in the early centuries of historical times (Larsen, 1984). Since 1974, the Bárðarbunga area has been the centre of unusual seismic activity with the occurrence of ten large earthquakes ($M_w \geq 5.1$), the latest having occurred prior to the large volcanic eruption in September 1996 (Einarsson, 1991; Nettles and Ekström, 1998). The epicentres are located around the Bárðarbunga caldera and their focal mechanisms appear to deviate from the double-couple source model.

In this paper, we present the results of the analysis of data recorded during the main phase (September 29–October 6) of the 1996 eruption, by a temporary (HOTSPOT) and a permanent seismic network (SIL). Our study starts with the location of the events and their spatial and temporal distribution, using all available data from both networks. We then examine the nature of the recorded seismic signals in the time and frequency domain in an effort to correlate them with the evolution of the eruption. Of particular interest is the occurrence of volcanic tremor before the main phase of the eruption, as well as its spectral characteristics, indicating again the potential importance of tremor in volcanic hazard assessment (Aki, 1992).

2. Data collection and analysis

In the summer of 1996, the HOTSPOT network was installed in Iceland as a joint project of Princeton and Durham Universities, the Icelandic Meteorological Office and the US Geological Survey. The primary purpose of the project was to obtain high quality data of local and teleseismic events in order to study the crustal and mantle structure, as well as to monitor the volcanic and high-seismicity zones. HOTSPOT consisted of 30 stations (Fig. 2) equipped with broadband three-component CMG3-ESP instruments, that

Table 2
Crustal model used to locate events

Layer thickness (km)	<i>P</i> wave velocity (km s ⁻¹)
1.00	3.53
2.00	4.47
3.00	5.16
4.00	5.60
6.00	5.96
9.00	6.50
20.00	6.73
32.00	7.20
90.00	7.40

had a flat velocity response in the frequency range of 0.03–20 Hz and Refraction Technology 72a-02 16-bit data loggers recording continuously at a rate of 20 samples s⁻¹. Absolute timing was provided by GPS receivers. The data were stored on disks which were changed every 1–4 months. HOTSPOT remained in operation until August 1998. Throughout the main phase of the 1996 eruption, all the HOTSPOT stations were operational except from HOT26. The SIL (South Iceland Lowlands) network (Stefánsson et al., 1993) is a permanent network consisting of 30 stations with broadband or short period sensors, recording data using a triggering mechanism. It is operated by the Icelandic Meteorological Office and its stations are mainly concentrated on the South Iceland Seismic Zone and the Tjörnes fracture zone in the north, where the seismic hazard is higher.

We started analysing the HOTSPOT data first by identifying events that were recorded by at least five stations, with a good azimuthal coverage around the eruption site and with high signal-to-noise ratio. Arrival times were manually picked and each pick was assigned a quality value, which was in most cases 1 for a P wave and 3 for an S wave pick (using 0 as best quality and 4 as worst). In this way, our final dataset for the eight days period consisted of 339 events. Earthquakes were located using the program *gloc* (B.R. Julian, pers. commun., 1998), which performs an iterative, damped inversion of arrival time data from each recording station to minimise the sum of the travel time residuals. The one-dimensional (1D) crustal model (Table 2) we used is based on the results of the tomographic study of Iceland by Bjarnason et al. (1993).

Arrival times from the SIL stations were added to

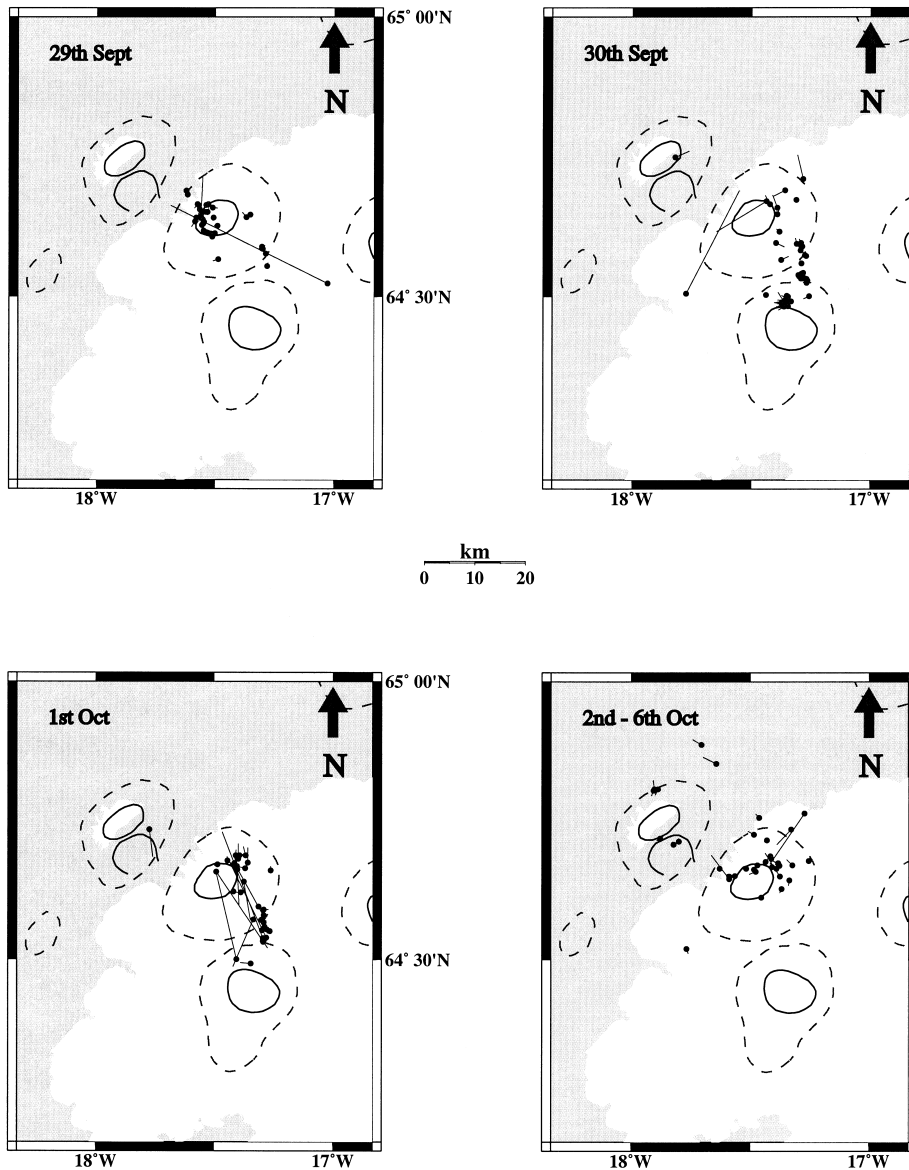


Fig. 3. Maps of events relocated using both HOTSPOT and SIL arrival times. The relocation vector has a direction from the location obtained with HOTSPOT arrival times to the new location obtained with HOTSPOT and SIL arrival times (black circle).

the HOTSPOT picked times, doubling the number of picks for each event, thus giving us the opportunity to estimate error bounds in our initial locations. However, due to the difference in detection thresholds, this was possible only for the events recorded by both networks. The relocation map for these events (Fig. 3) shows for most cases a difference in the

epicentre locations of ± 1 km. Larger differences are the result of the difficulty in picking small events with very emergent P onsets, introducing larger errors in the measurement of the arrival times. Residual values were usually less than 0.5 and 0.8 s for the P and S picks, respectively.

As in previous studies of the seismicity of the

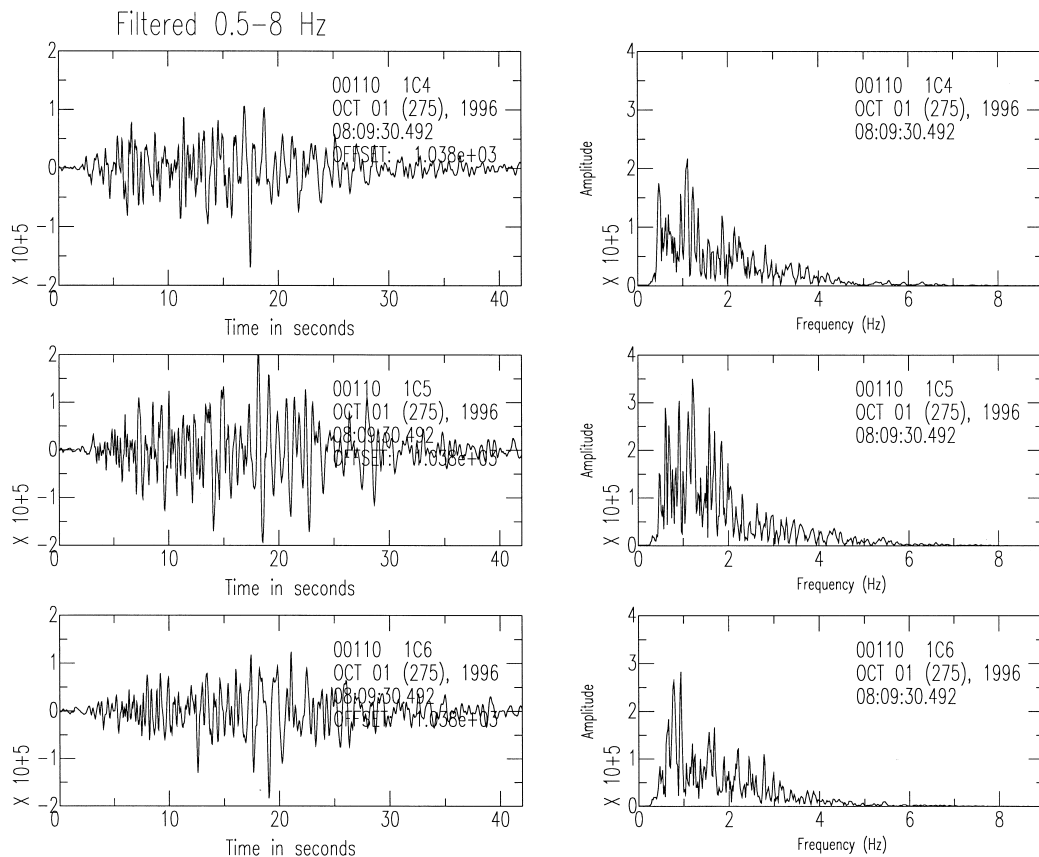


Fig. 4. Velocity waveforms and amplitude spectra of a low-frequency event recorded after the onset of the subglacial eruption (October 1) at station HOT23 by a three-component seismometer. The amplitude scales are normalised to the largest value of the three components. 1C4: vertical component, 1C5: north–south component, 1C6: east–west component.

area (Einarsson and Brandsdóttir, 1984), we had a difficulty in constraining the hypocentral locations for a large number of events. The main reason for this is the poor knowledge of the strongly heterogeneous Icelandic crust, which cannot be represented by a 1D velocity model. Currently, efforts are under way to determine a 3D model for the Iceland crust, using surface waves (Allen et al., 1999) and receiver functions (Z.J. Du, pers. commun., 1998) and may solve this problem in the future. A secondary reason is the lack of clear S phases from most of the events. Taking into account the thinning of the upper crust beneath Vatnajökull, as indicated by seismic refraction studies (Darbyshire et al., 1998), we have chosen to include only those hypocentres which are located no deeper than 8 km.

3. Description of seismic signals

Most of the seismic signals recorded during the eight-day period of the main eruption were categorised into groups based on waveform appearance and frequency content. Many classification schemes for volcanoseismic phenomena (e.g. Lahr et al., 1994) try to utilise these two criteria to interpret source processes. However, this can be a very difficult task, taking into account the complicated and poorly known velocity structure of most volcanic areas around the world, that can distort many features of the original waveform. In order to avoid this complicating factor, we group events using terms that are descriptive of the waveform and amplitude spectrum and not of the underlying source process. We summarise below the characteristics of each of these groups.

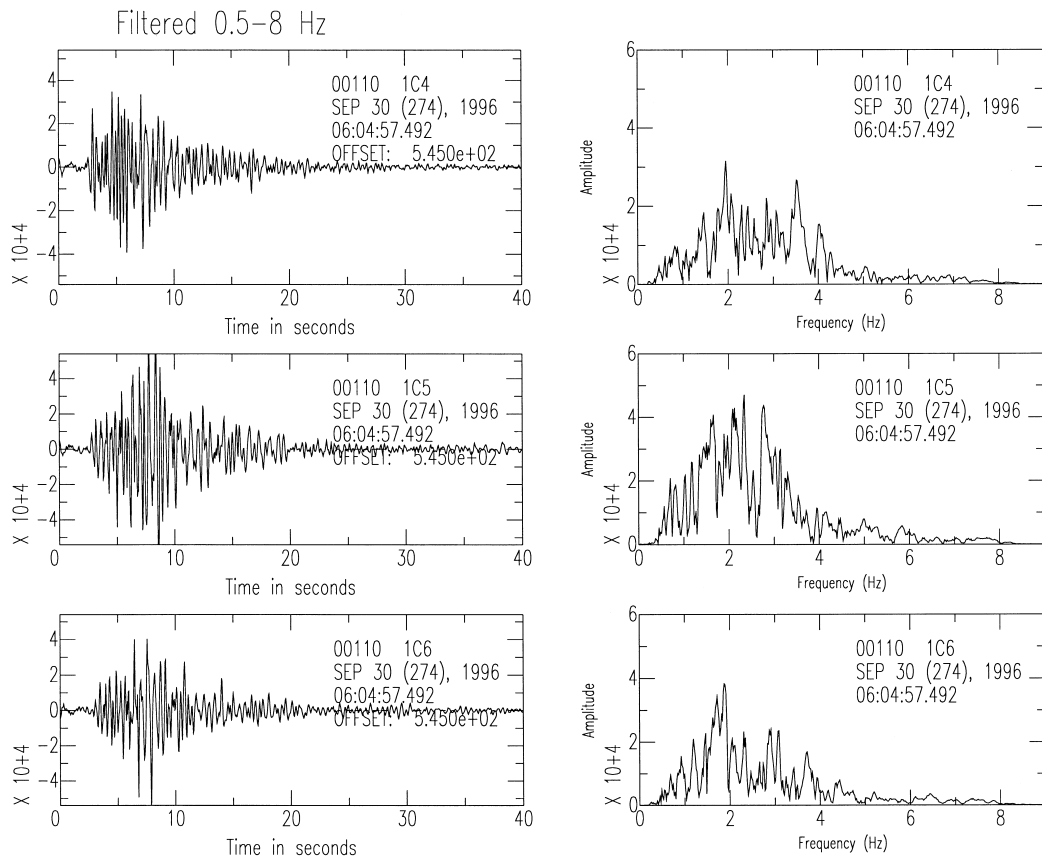


Fig. 5. Same as in Fig. 4, for a mixed-frequency event, recorded before the onset of the eruption. Note the impulsive high-frequency onset and how the coda decays exponentially with time, decreasing the duration of the signal, to about half of that of the low-frequency event in the previous figure.

Low-frequency events. The waveform is characterised by an emergent onset of the P wave and lack of clear S phases. The coda decays very slowly with time, increasing the duration of the signal up to 1 min. The energy in the spectrum is mostly in the range 0.5–2 Hz, with multiple sharp peaks (Fig. 4). In many cases, two or more of these events are clustered together forming a continuous wavetrain.

Mixed-frequency events. The waveform is characterised by a high frequency, impulsive P wave onset followed by a coda that decays almost exponentially with time. There is considerable energy in the range 1–2 Hz, but energy at higher frequencies is also present (Fig. 5).

Volcanic tremor. Following the start of the eruption,

wavetrains with small amplitudes form continuous background tremor. Tremor bursts with larger amplitudes and variable duration are superimposed on it (Fig. 6). Energy is concentrated in the frequency range 0.5–3.9 Hz.

4. Spatio-temporal variations of seismicity

At 10:48 h GMT on the morning of September 29, an earthquake of magnitude $M_w = 5.6$ took place near the northern rim of the Bárðarbunga caldera (Fig. 7). It was followed by a swarm of other earthquakes about 20 min later. All of these earthquakes may be characterised as low-frequency events and their epicentres

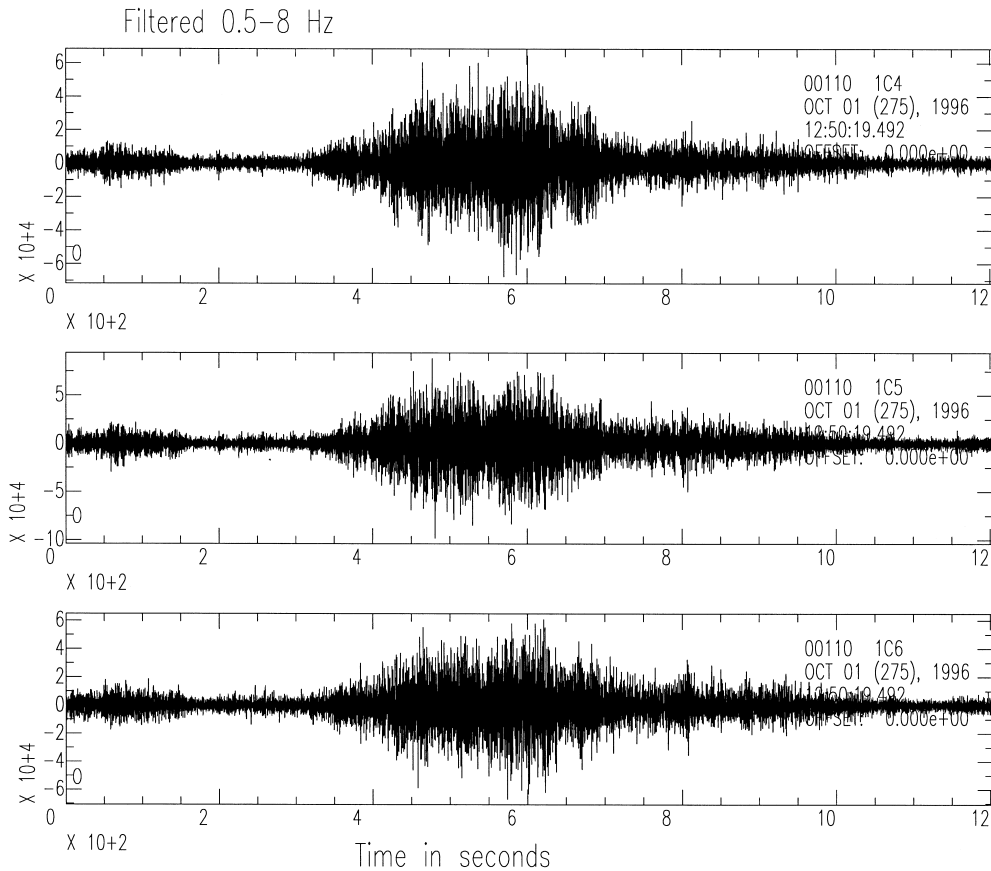


Fig. 6. Waveforms of high-amplitude tremor superimposed on the background tremor, recorded after the subglacial eruption (October 1) at station HOT23.

delineate the caldera rim. Between 14:10 and 17:20 h, the activity decreased and resumed again in the evening of the same day. This time the epicentres were located to the SE of the Bárðarbunga caldera and 15 km away from the area where the seismic activity first started. The spectra of these events exhibit energy at higher frequencies but the coda decays slowly, like those of low-frequency events.

In the early hours of morning, the seismic activity continued at the same area, slowly migrating southwards towards Grimsvötn during the day (Fig. 8). The resulting earthquake cluster that is formed is elongated in the NNE–SSW direction and covers the same area where the eruptive fissure and depressions on the ice were observed later. Meanwhile, the Bárðarbunga area was relatively quiet, with only a few events occurring at the NE

caldera rim. Almost all of these earthquakes are mixed-frequency events that have a coda decaying exponentially with time. Later that evening (22:00) continuous volcanic tremor started being visible above the ambient background noise at the nearest station (HOT23), indicating that the subglacial eruption was imminent.

On October 1, the activity persisted in the northern part of Grimsvötn, forming a smaller elongated cluster of epicentres, while at the same time another cluster formed at the NE part of the Bárðarbunga area (Fig. 9). Early in the morning of that day, the fissure and depressions in the ice were observed from an aeroplane. Most of the earthquakes recorded subsequently are typical low-frequency events, superimposed on the background tremor. On October 2, the eruption broke through the ice and became subaerial, but the

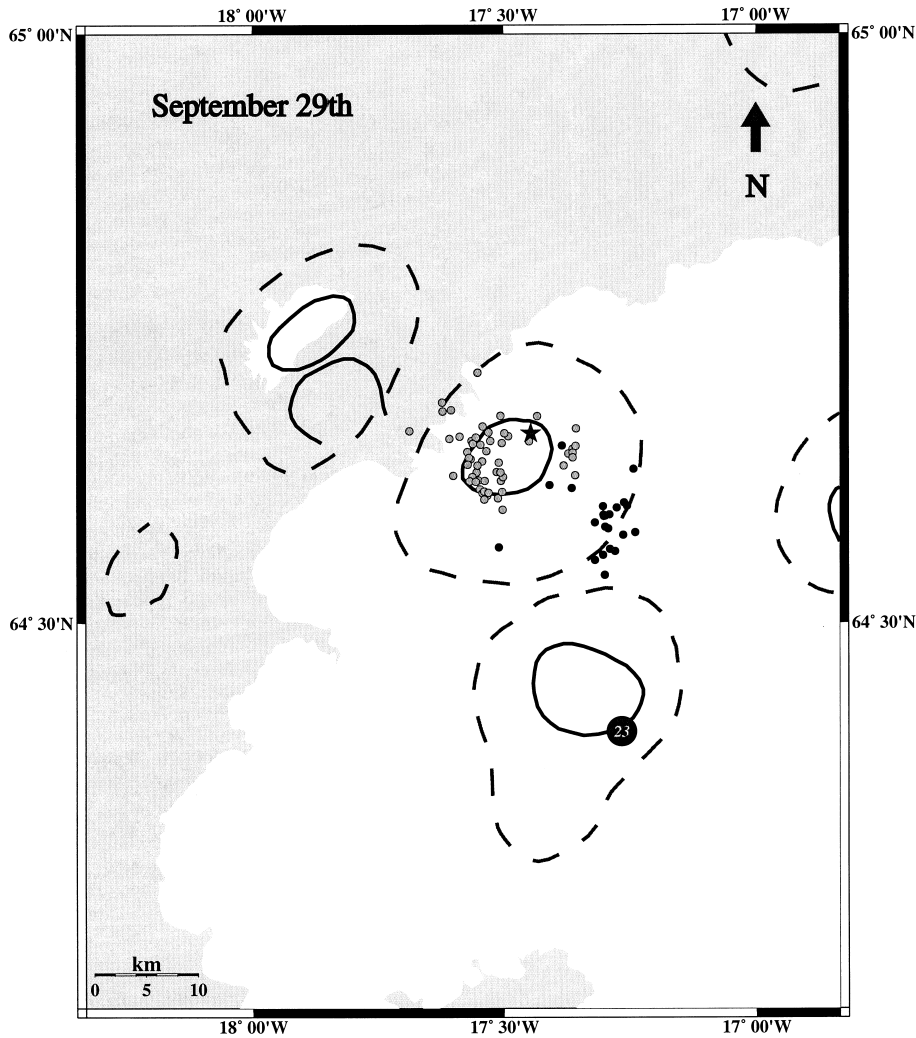


Fig. 7. Map of events located by HOTSPOT for September 29. The star indicates the epicentre of the magnitude $M_w = 5.6$ event at Bárðarbunga. The grey circles indicate epicentres of low-frequency events, while the black indicate epicentres of mixed-frequency events.

seismic activity decreased considerably. The Grimsvötn area was quiet and most of the events were located in the NE part of the Bárðarbunga caldera (Fig. 10). On subsequent days (October 3–6), low-frequency events continued to take place in the NE of Bárðarbunga and inside its caldera. However, a small number of earthquakes was located to the north and inside Tindafjallajökull volcanic system, up to 20 km away from the Bárðarbunga caldera (Fig. 11). Cross-sections of the hypocentres for the whole period are shown in Fig. 12.

5. Spectral analysis of volcanic tremor

Volcanic tremor was first observed at the nearest station to the eruption site (HOT23) in the evening of September 30 and was recorded continuously for 14 days, until the afternoon of October 13. Our study of the spectral characteristics of tremor covers the whole of this period, in an effort to check whether there was any substantial seismic activity shortly before the main eruption. In order to be able to observe better the temporal variations in the

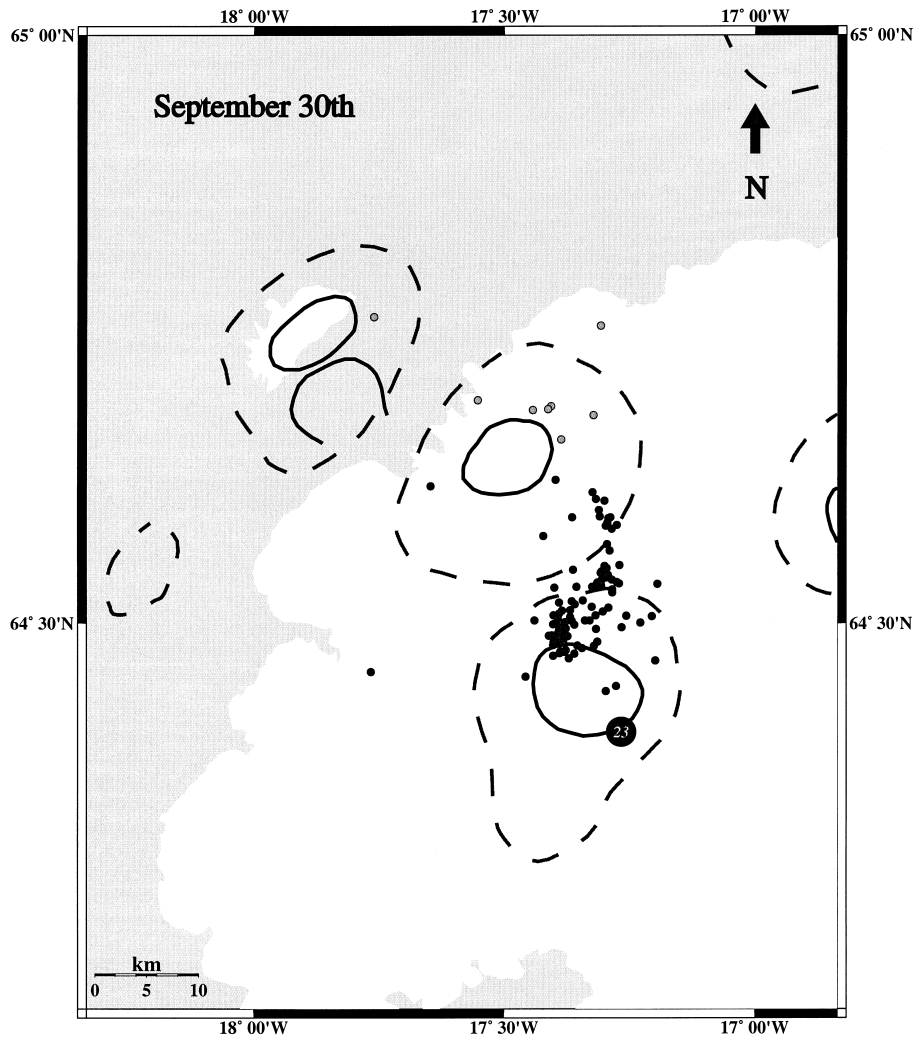


Fig. 8. Same as Fig. 7, for September 30.

frequency content of tremor, we created spectrograms for each of the three components of station HOT23 over successive time intervals of 12 h. A spectrogram is simply a 2D representation of the variations of spectral energy and frequency of the observed signal as time elapses.

The spectrograms for the first day revealed the existence of a seismic signal around five narrow frequency bands of 0.5–0.7, 1.6, 2.2, 2.8 and 3.2 Hz, not clearly visible on all three components (Fig. 13). This signal continued to be present in the spectrogram of the next day but there was an abrupt

reduction in amplitude about 5 h before the large earthquake at Bárðarbunga occurred (Fig. 14). It is interesting to note the numerical relationship of the above values: there are peaks at fundamental frequencies of 3.2, 2.8 and 2.2 Hz with corresponding subharmonics at 1.6, 0.7 and 0.55 Hz, respectively. For the following day (September 30), it is quite difficult to decipher any of these frequency bands, due to the large number of earthquakes occurring in the same range of frequencies. For the remaining period up to the day that tremor was last recorded (October 13), the same pattern is observed,

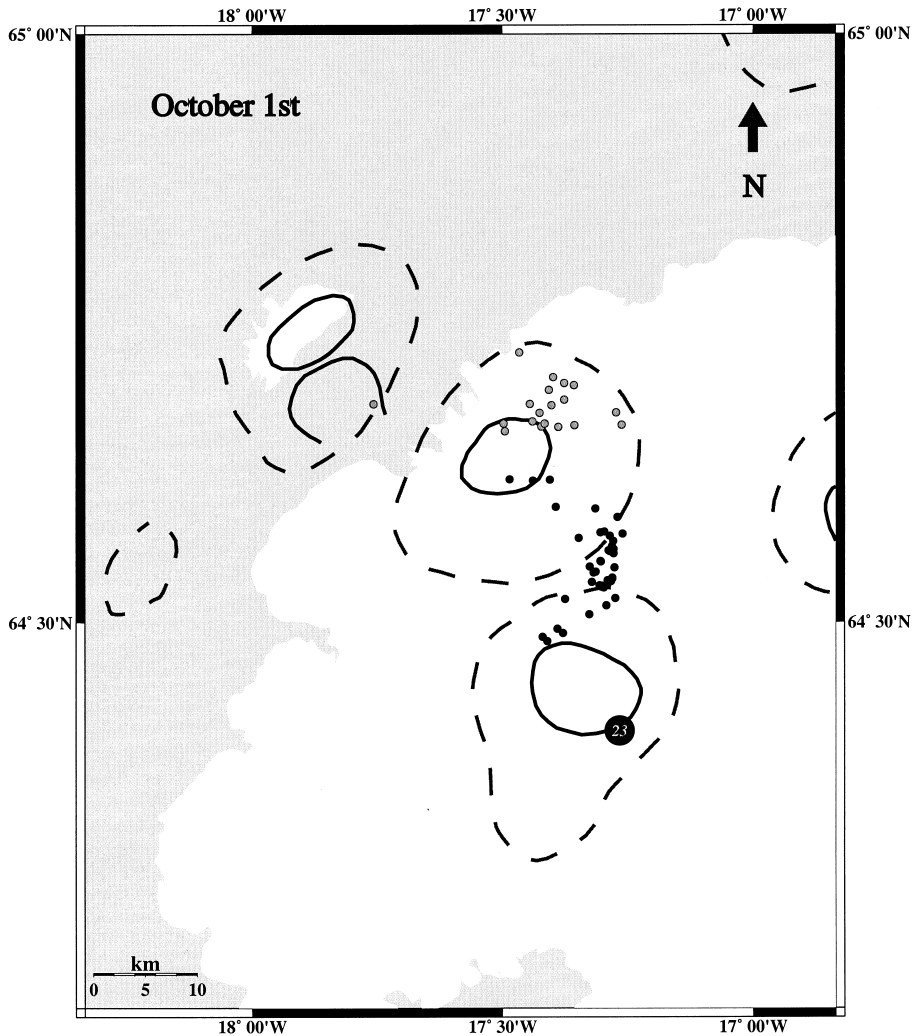


Fig. 9. Same as Fig. 7, for October 1.

with the appearance of the same fundamental frequencies and their half- and quarter-subharmonics (Fig. 15).

Such behaviour, where the period of the tremor signal is doubled, has also been observed at other volcanoes, e.g. in Hawaii (Aki and Koyanagi, 1981), Mt Semeru, Indonesia (Schlindwein et al., 1995) and Arenal volcano, Costa Rica (Barquero et al., 1992) and is believed to be the result of increasing nonlinearity in the source. This nonlinear process can be modelled numerically considering the flow of magmatic fluids through a constricted channel with

deformable walls (Julian, 1994). Depending on the physical properties of the fluid-walls system and the variations of the fluid pressure, there can be either steady flow with no wall oscillations or cycles of opening and closing of the channel walls, responsible for the phenomenon of period doubling.

6. Discussion

The 1996 eruption at the Vatnajökull glacier was accompanied by a variety of seismic and volcanic

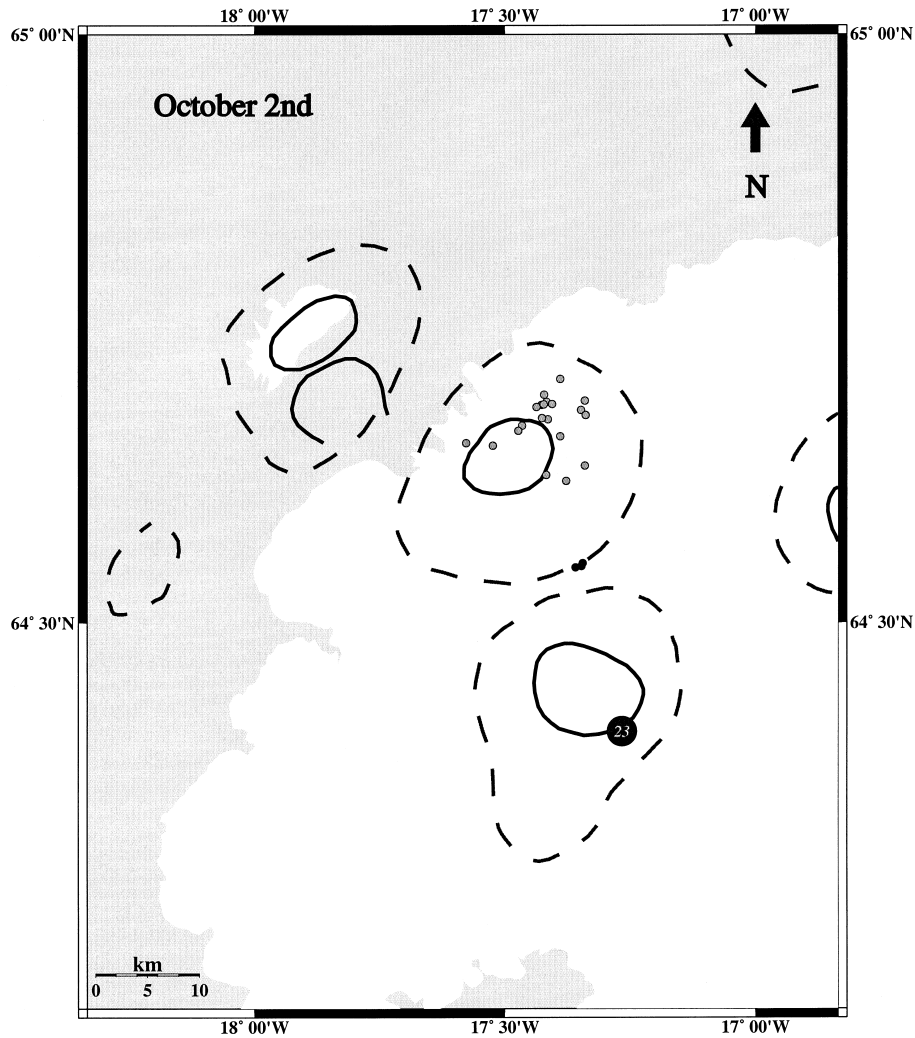


Fig. 10. Same as Fig. 7, for October 2.

phenomena, affecting a much larger area than just the area between Bårdarbunga and Grimsvötn and more than one volcanic system. While other volcanoes in Iceland may erupt without any precursory activity, e.g. the Hekla eruptions in 1970, 1980, 1981 and 1991 (Brandsdóttir and Einarsson, 1992), this eruption was preceded by a series of remarkable precursory phenomena. Examination of the seismicity of this area for a period of four and a half years before the eruption (Fig. 16a) revealed a considerable increase in seismic activity during the first half of 1996 in the nearby Hamarinn volcano. This is in accordance

with earlier observations, which indicate that seismic activity in Hamarinn may affect Bårdarbunga and vice versa (Björnsson and Einarsson, 1990).

Our analysis also revealed short-term precursors, in the form of volcanic tremor signals, approximately two days before the main eruption and just before the onset of the episodic earthquake swarm that preceded it (Fig. 16b). Based on the spectral characteristics of the signals, we can interpret them as evidence of flow of magma from a deeper source to a shallow magmatic chamber beneath Bardarbunga. Studies of the crustal structure beneath other Icelandic

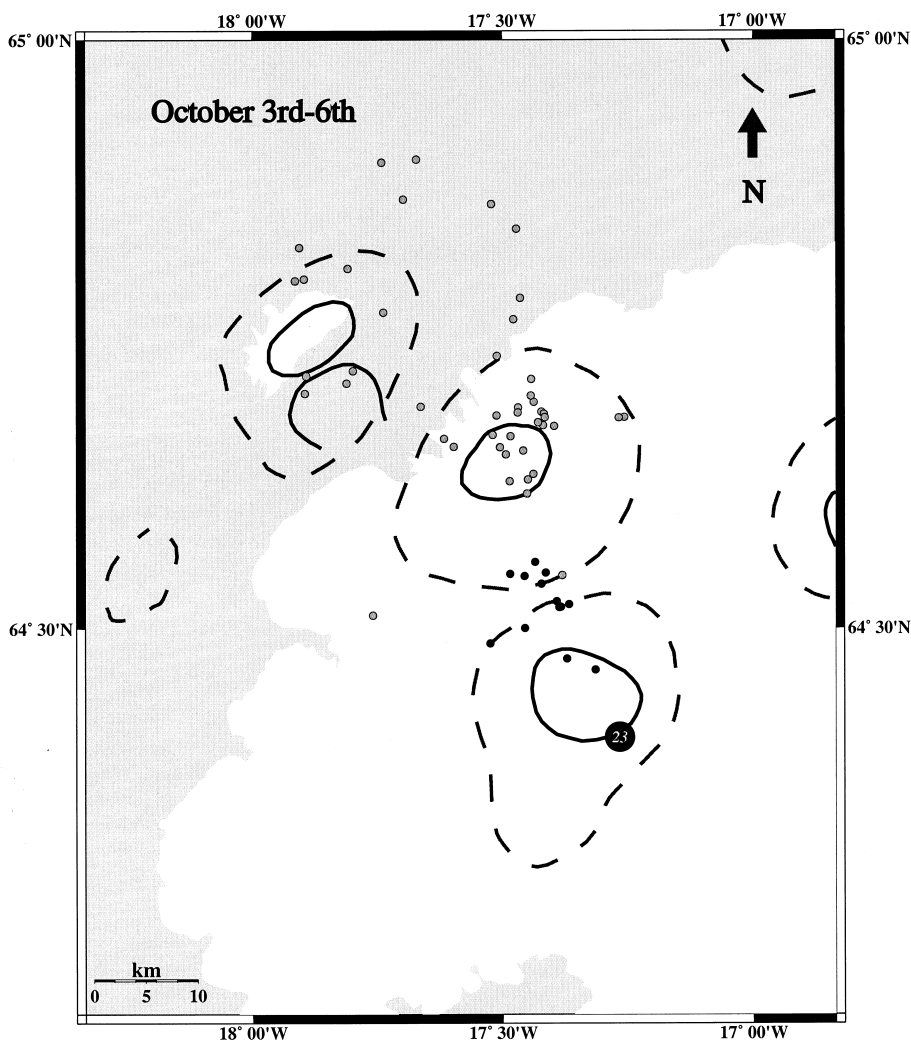


Fig. 11. Same as Fig. 7, for the period October 3–6.

volcanoes have revealed that magma chambers, filled with partially molten material, exist at depths of 1–3 km (Einarsson, 1978; Gudmundsson et al., 1994; Gudmundsson, 1995).

The large earthquake that followed the pre-eruptive tremor signals had all the characteristics of a typical low-frequency event and its focal mechanism showed a large deviation from the conventional double couple model. Nettles and Ekström (1998) obtained the centroid moment tensor solution for this event, using teleseismic data. They interpreted its non-double couple nature as the result of thrust motion

on planes of varying strike that form an outward dipping cone-shaped ring fault beneath the Bárðunga caldera. The fact that the epicentres of the earthquakes that followed form a curved line along the western caldera rim (Fig. 7) may be evidence for such a rupture process. Numerical studies of the stress field around shallow magma chambers indicate that the initiation of ring faults is possible for sill-like magma chambers affected by doming of an area much larger than that of their caldera (Gudmundsson et al., 1997). This agrees well with the observations of early activity in Hamarinn and the shifting of

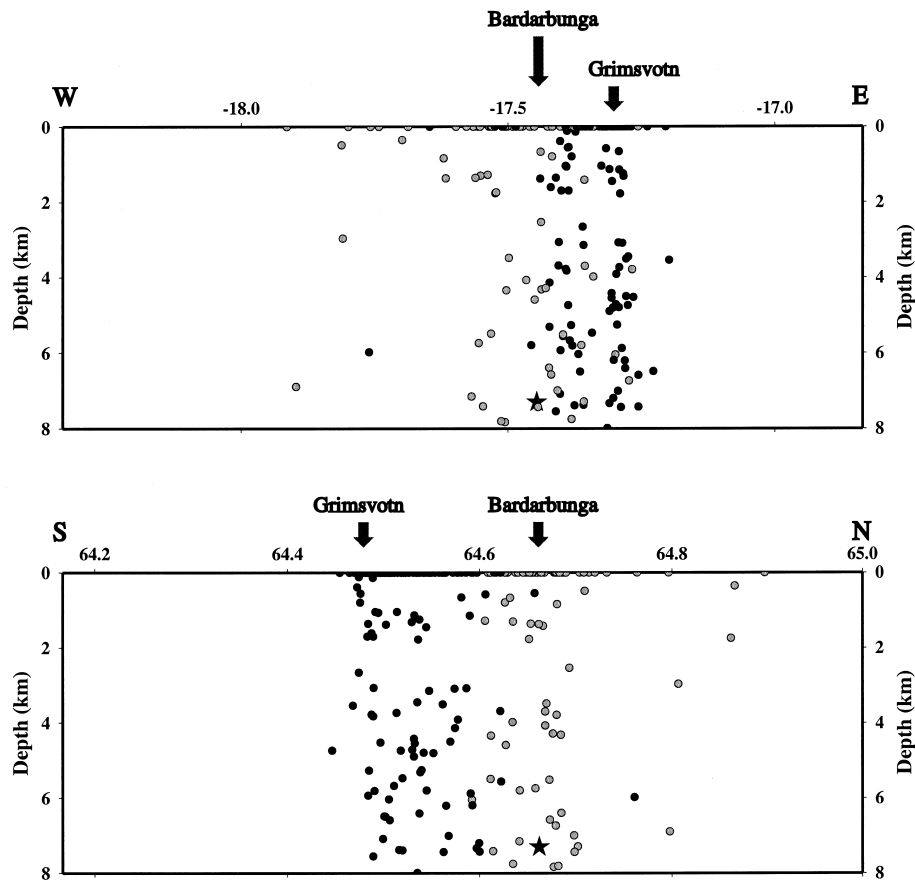


Fig. 12. East–west and north–south depth cross-sections of events for the period September 29–October 6. Symbols as in Figs. 7–11.

seismicity towards Tindafjallajökull during October 3–6. Also the shift of the epicentres that we observed in September 29–30 towards Grimsvötn and the formation of a fissure at the same place may suggest a lateral migration of magma from the shallow chamber underneath Bárðarbunga.

An alternative explanation for a non-double couple mechanism and for the course of events during the eruption, is that of a dyke injection below an area close to the eruptive site (R. Stefánsson, personal communication, 1999). It is believed that such a process had been going on in that area for a period of approximately 10 years and that the earthquakes were releasing compressive stress caused by dyke injection below the Vatnajökull area. Similar processes are believed to have taken place in other volcanoes around the world, accompanied by such

anomalous earthquakes, as in Long Valley caldera (Julian, 1983) and at the Izu-Oshima volcano, Japan (Ukawa and Ohtake, 1987). In the case of Icelandic volcanoes a well-documented example of long-term dyke intrusion is the rifting episode at Krafla volcano in 1975–1984 (Brandsdóttir and Einarsson, 1979). Earthquakes with non-double couple characteristics are the result of concentrated tensile stress in the area where magma is forcing its way to the upper parts of the crust. Research is under way to obtain more focal mechanism solutions of earthquakes following the large event at Bárðarbunga that will allow a more thorough assessment of the physical mechanism of the eruption than it is possible with the analysis presented here.

Volcanoseismic phenomena have not previously been so well recorded in such an active area as NW

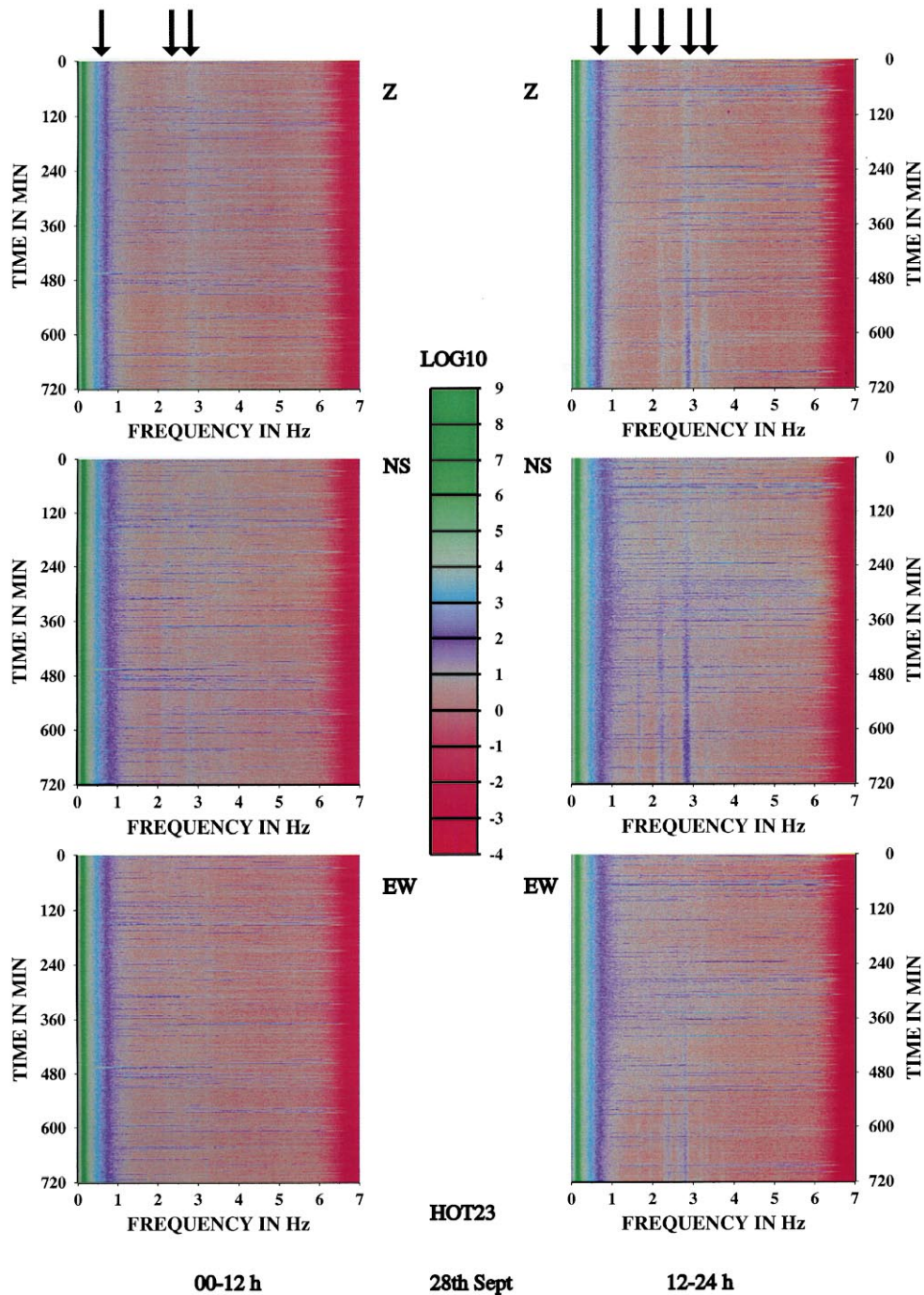


Fig. 13. Tremor spectrograms for September 28. Each plot represents 12 h of data for the three components of station HOT23. The colour scale for the amplitude is logarithmic. Vertical arrows show the frequency bands observed. The high-amplitude signal below 0.3 Hz represents ocean microseismic noise.

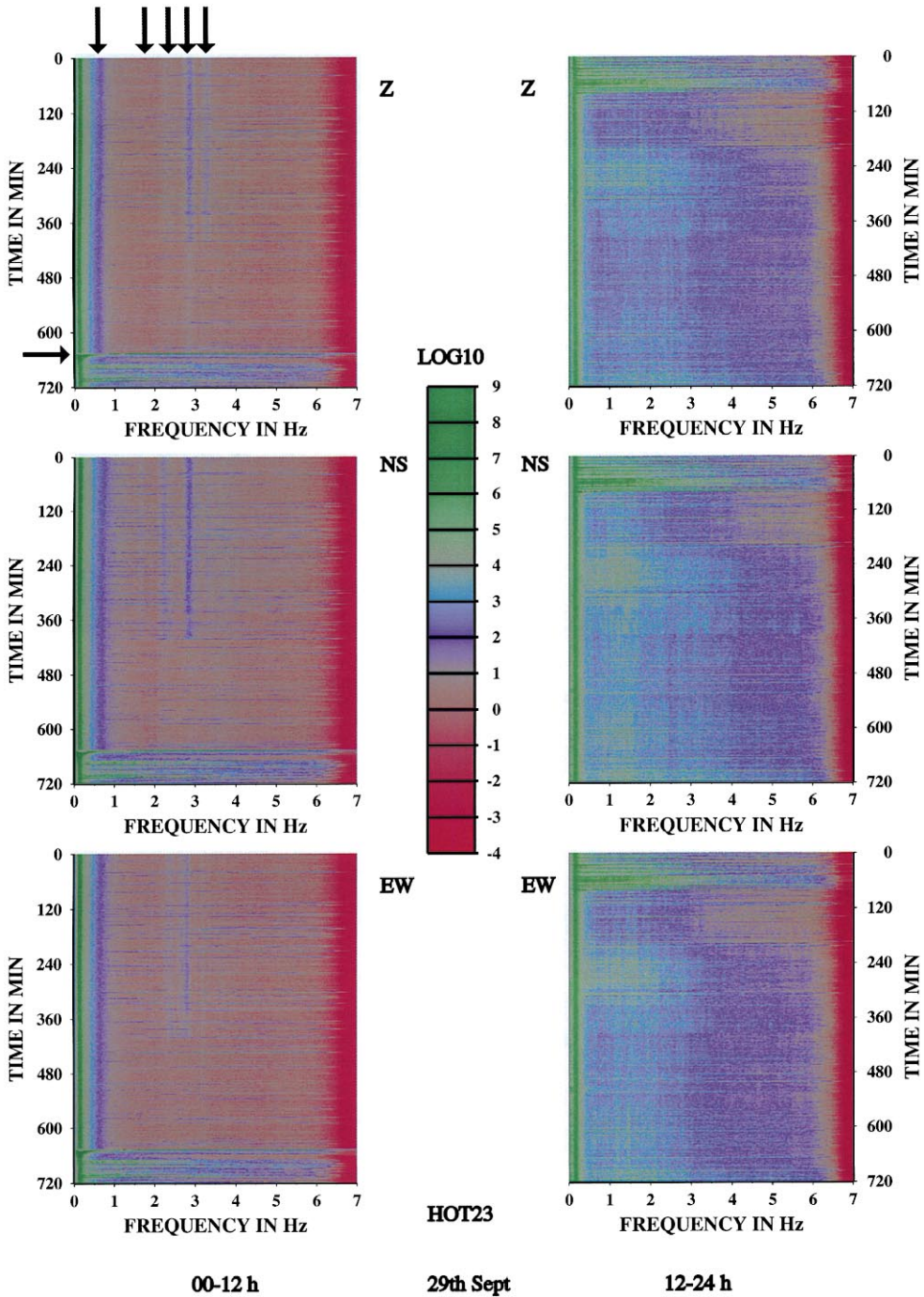


Fig. 14. Same as Fig. 13, for September 29. Horizontal arrow shows the onset of the large event at Bardarbunga and the swarm that followed it.

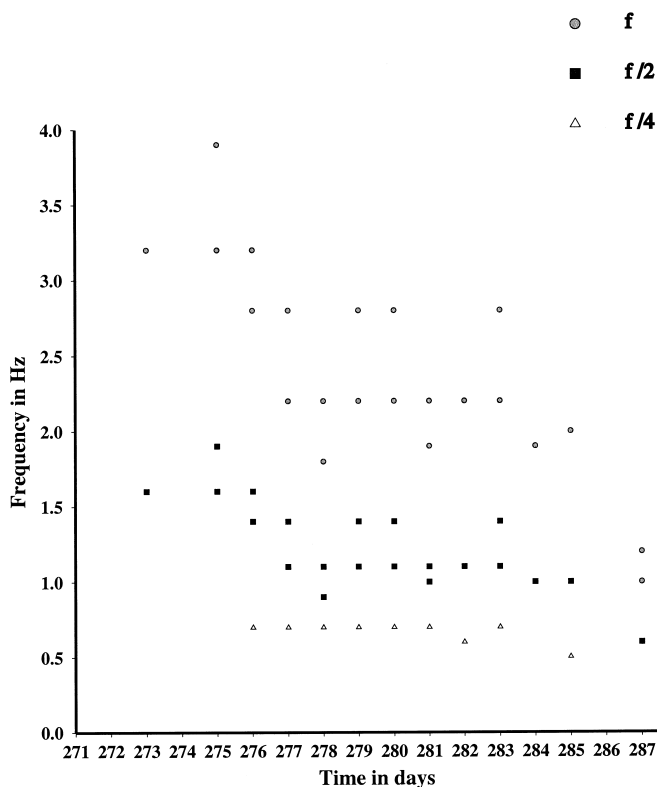


Fig. 15. Diagram of frequency versus time, showing the fundamental frequencies and their half- and quarter-subharmonics for each day, from September 28 (272) to October 13 (287).

Vatnajökull. The scientific observations described in this paper show once again the significant role that seismic monitoring of active volcanoes can play in the successful identification of eruption precursors. However, apart from the social benefit of eruption forecasting, seismic monitoring also provides an opportunity of obtaining a more thorough understanding of the processes inside active volcanoes.

Acknowledgements

We would like to thank Neil Goulty, Vera Schlindwein, Prof. Roger Searle and an anonymous reviewer for reading this manuscript and contributing many helpful suggestions. We would also like to thank Ragnar Stefansson, members of staff at the Icelandic Meteorological Office and Kristin Vogfjörð for useful discussions and for sharing data and information with

us. Christine Peirce kindly provided financial support for the reproduction of coloured figures 13–14. The HOTSPOT project was funded by the National Environmental and Research Council (NERC) grants GST/02/1238 and GR3/10727 held by G.R. Foulger, NSF grant EAR 9417918 and supported by the US Geological Survey. We thank IRIS/PASSCAL for technical support and assistance in running the network. All the maps and diagrams in this paper were plotted using the GMT software package (Wessel and Smith, 1995), the figures containing waveforms and spectra were produced using SAC2000 (Goldstein et al., 1998) and the software used to create the spectrograms was written by B.R. Julian. More information about the 1996 and 1998 eruptions in Vatnajökull, as well as a database containing preliminary determined parameters of earthquakes located by the SIL network, can be found at the Icelandic Meteorological Office webpage: <http://www.vedur.is>

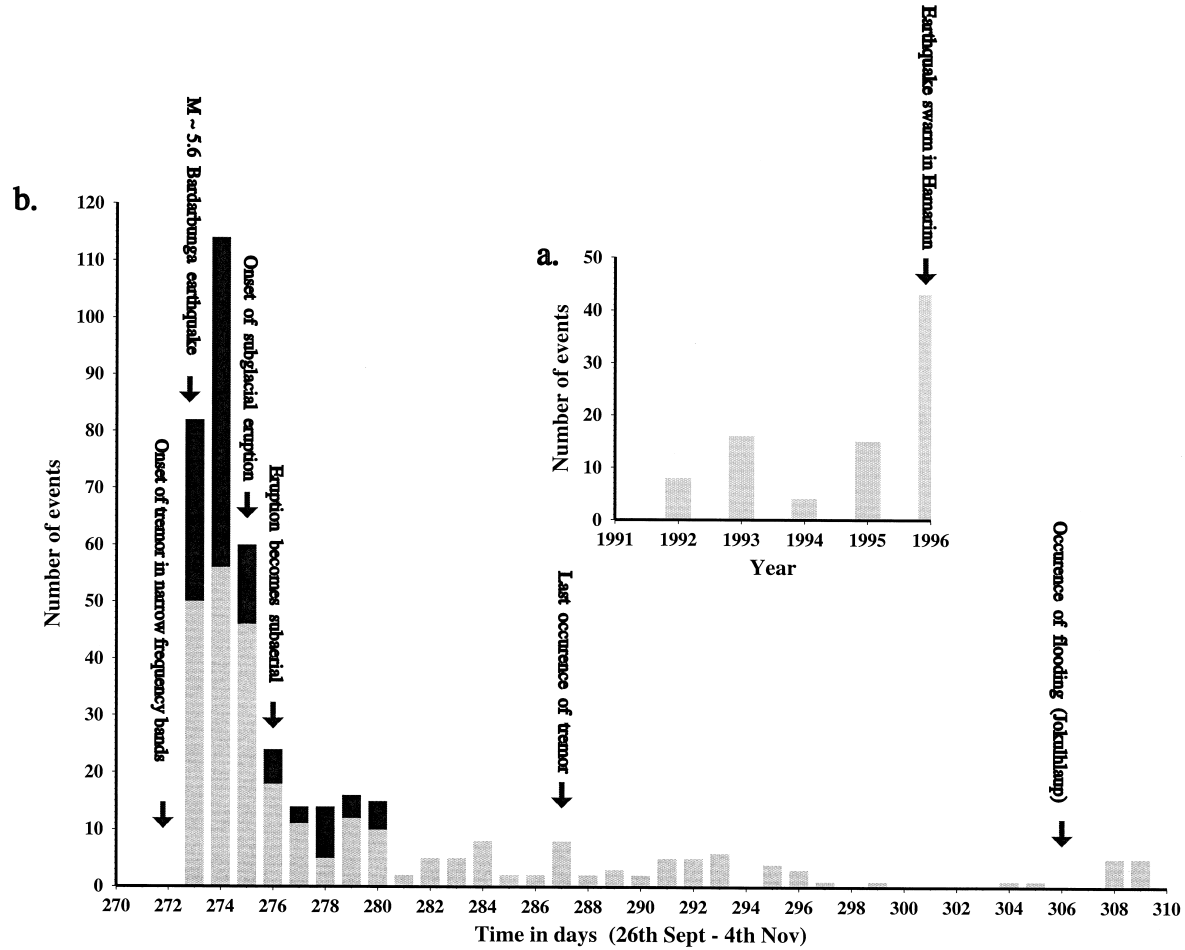


Fig. 16. (a) Annual seismicity levels from 1992 to September 1996 (numbers were obtained from the SIL network database) (b) Histogram showing the distribution of located events during the whole period of the eruption. Black bars: events located using only HOTSPOT data, grey bars: events located using only SIL data.

References

- Aki, K., 1992. State of the art in volcanic seismology. In: Gasparini, P., Scarpa, R., Aki, K. (Eds.), *Volcanic Seismology*. IAVCEI Proceedings in Volcanology, vol. 3, pp. 3–10.
- Aki, K., Koyanagi, R.Y., 1981. Deep volcanic tremor and magma ascent mechanism under Kilauea, Hawaii. *J. Geophys. Res.* 86, 7095–7110.
- Allen, R.M., et al., 1999. Toward a 3D crustal S-velocity model for Iceland. *EOS Trans. AGU* 80 (17), S220 (Spring Meet suppl.).
- Barquero, R., Alvarado, G.E., Matumoto, T., 1992. Arenal volcano (Costa Rica) premonitory seismicity. In: Gasparini, P., Scarpa, R., Aki, K. (Eds.), *Volcanic Seismology*. IAVCEI Proceedings in Volcanology, vol. 3, pp. 3–10.
- Brandsdóttir, B., Einarsson, P., 1979. Seismic activity associated with the September deflation of the Krafla central volcano in NE Iceland. *J. Volcanol. Geotherm. Res.* 6, 197–212.
- Brandsdóttir, B., Einarsson, P., 1992. Volcanic tremor and low-frequency earthquakes in Iceland. In: Gasparini, P., Scarpa, R., Aki, K. (Eds.), *Volcanic Seismology*. IAVCEI Proceedings in Volcanology, vol. 3, pp. 212–222.
- Bjarnasson, I.T., Menke, M., Flóvenz, O.G., Caress, D., 1993. Tomographic image of the Mid-Atlantic plate boundary in southwestern Iceland. *J. Geophys. Res.* 98, 6607–6622.
- Björnsson, H., 1988. Hydrology of ice caps in volcanic regions. *Soc. Sci. Isl. Reykjavik* 45, 139.
- Björnsson, H., Einarsson, P., 1990. Volcanoes beneath Vatnajökull, Iceland: evidence from radio echo-sounding, earthquakes and jökulhlaups. *Jökull* 40, 147–167.
- Darbyshire, F.A., Bjarnason, I.T., White, R.S., Flóvenz, O.G., 1998. Crustal structure above the Iceland mantle plume imaged by the ICEMELT refraction profile. *Geophys. J. Int.* 135, 1131–1149.
- Einarsson, T., 1954. A survey of gravity in Iceland. *Visindafelag Isl. Rit.* 30, 22.
- Einarsson, P., 1978. S-wave shadows in the Krafla caldera in NE-Iceland: evidence for a magma chamber in the crust. *Bull. Volcanol.* 41, 1–9.
- Einarsson, P., 1991. Earthquakes and present-day tectonism in Iceland. *Tectonophysics* 189, 261–279.
- Einarsson, P., Brandsdóttir, B., 1984. Seismic activity preceding and during the volcanic eruption Grimsvötn, Iceland. *Jökull* 34, 13–23.
- Goldstein, P., Dodge, D., Firpo, M., Ruppert, S., 1998. What's new in SAC2000? Enhanced processing and database access. *Seismol. Res. Lett.* 69, 202–205.
- Gudmundsson, A., 1995. Infrastructure and mechanics of volcanic systems in Iceland. *J. Volcanol. Geotherm. Res.* 64, 1–22.
- Gudmundsson, M.T., 1989. The Grimsvötn caldera, Vatnajökull: subglacial topography and structure of caldera infill. *Jökull* 39, 1–20.
- Gudmundsson, M.T., Björnsson, H., 1991. Eruptions in Grimsvötn, Vatnajökull, Iceland, 1934–1991. *Jökull* 41, 21–42.
- Gudmundsson, O., Brandsdóttir, B., Menke, M., Sigvaldason, G.E., 1994. The crustal magma chamber of the Katla volcano in south Iceland revealed by 2-D seismic undershooting. *Geophys. J. Int.* 119, 277–296.
- Gudmundsson, A., Marti, J., Turon, E., 1997. Stress fields generating ring faults in volcanoes. *Geophys. Res. Lett.* 24, 1559–1562.
- Jakobsson, S., 1979. Petrology of recent basalts of the eastern volcanic zone, Iceland. *Acta Nat. Isl.* 26, 103.
- Jakobsson, S., 1980. Outline of the petrology of Iceland. *Jökull* 29, 57–73.
- Joset, A., Holtzschcherer, J.J., 1954. Expedition Franco-Islandaise au Vatnajökull Mars–Avril 1951, Resultats des sondages seismic. *Jökull* 4, 1–32.
- Julian, B.R., 1983. Evidence for dyke intrusion earthquake mechanisms near Long Valley caldera, California. *Nature* 303, 323–325.
- Julian, B.R., 1994. Volcanic tremor: nonlinear excitation by fluid flow. *J. Geophys. Res.* 99, 11 859–11 877.
- Larsen, G., 1984. Recent volcanic history of the Veidivötn fissure swarm, southern Iceland—an approach to volcanic risk assessment. *J. Volcanol. Geotherm. Res.* 22, 33–58.
- Lahr, J.C., Chouet, B.A., Stephens, C.D., Powers, J.A., Page, R.A., 1994. Earthquake classification, location, and error analysis in a volcanic environment: implications for the magmatic system of the – eruptions at Redoubt volcano, Alaska. *J. Volcanol. Geotherm. Res.* 62, 137–151.
- Nettles, M., Ekström, G., 1998. Faulting mechanism of anomalous earthquakes near Bárðarbunga volcano, Iceland. *J. Geophys. Res.* 103, 17 973–17 983.
- Schindwein, V., Wasserman, J., Scherbaum, F., 1995. Spectral analysis of harmonic tremor signals. *Geophys. Res. Lett.* 22, 1685–1688.
- Sigvaldason, G.E., Steinthorsson, S., Oskarsson, N., Imsland, P., 1974. Compositional variation in recent Icelandic tholeiites and the Kverkfjöll hotspot. *Nature* 251, 579–582.
- Stefánsson, R., Bödvarsson, R., Slunga, R., Einarsson, P., Jakobsdóttir, S., Bungum, H., Gregersen, G., Havskov, J., Hjelme, J., Korhonen, H., 1993. Earthquake prediction research in the south Iceland seismic zone and the SIL project. *Bull. Seismol. Soc. Am.* 83, 696–716.
- Sæmundsson, K., 1979. Fissure swarms and central volcanoes of the neovolcanic zones of Iceland. *Geol. J.* 19, 415–432.
- Sæmundsson, K., 1980. Outline of the Geology of Iceland. *Jökull* 29, 7–28.
- Tryggvason, K., Husebye, E.S., Stefánsson, R., 1983. Seismic image of the hypothesized Icelandic hotspot. *Tectonophysics* 100, 97–118.
- Ukawa, M., Ohtake, M., 1987. A monochromatic earthquake suggesting deep-seated magmatic activity beneath the Izu-Oshima volcano, Japan. *J. Geophys. Res.* 92, 12649–12663.
- Wessel, P., Smith, W.H.F., 1995. New version of the Generic Mapping Tools released. *EOS Trans. AGU* 76, 329.